Post-eruptive thermoelastic deflation of intruded magma in Usu volcano, Japan, 1992–2017

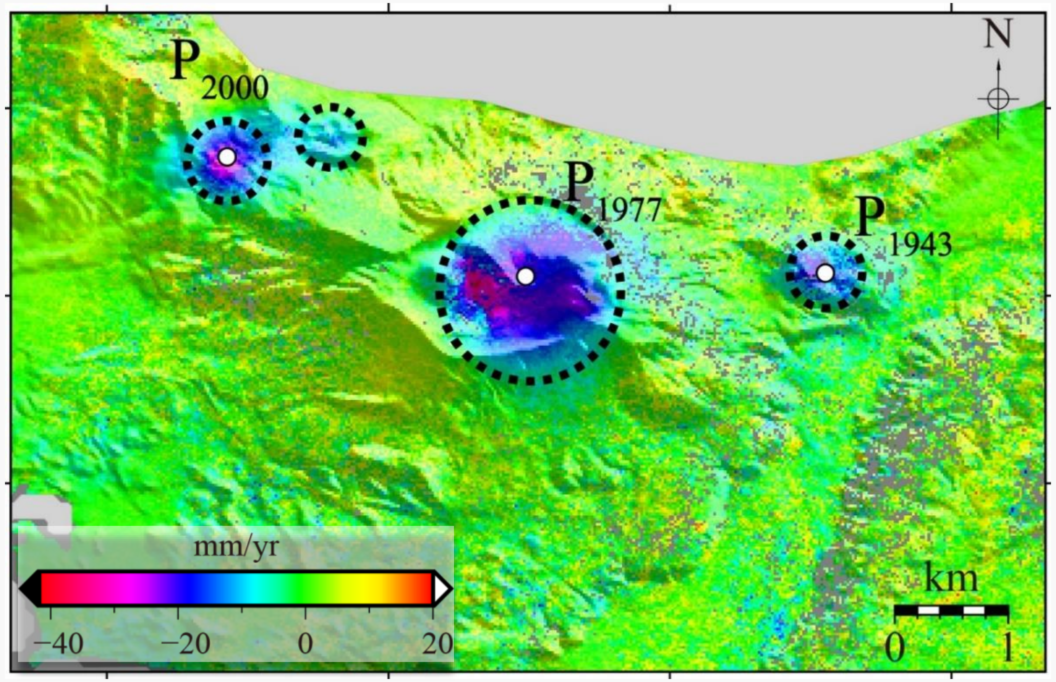

Xiaowen Wang, Yosuke Aoki

Earthquake Research Institute,

The University of Tokyo

Key Points:

- **InSAR shows three localized deformation regions**
- **Thermoelastic modeling reveals four shallow sources**
- **The modeling favors high thermal diffusivity**

Volcano deflation

Post-eruptive Subsidence

Parícutin, México
(*Chaussard, 2016*)

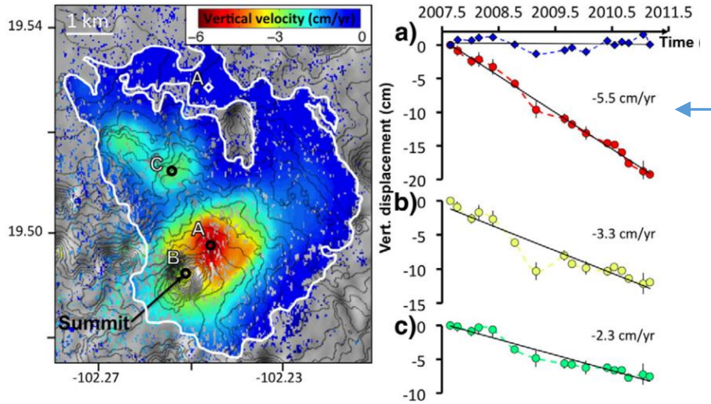

Kutcharo, Japan
(*Yamasaki et al., 2018*)

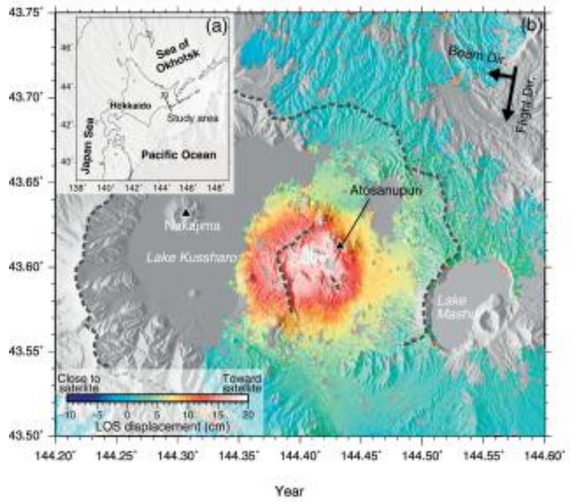

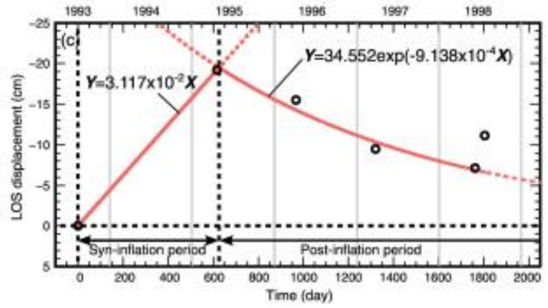

Nabro, Afar region
(*Hamlyn et al., 2018*)

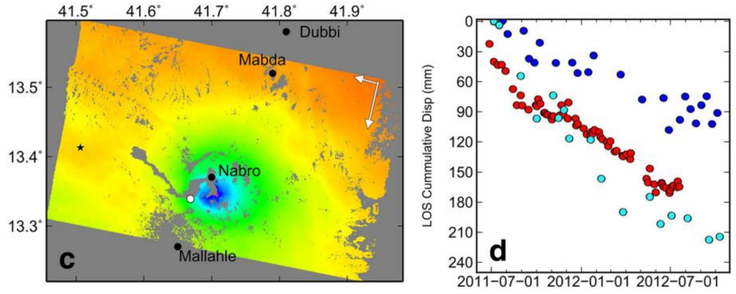

Nyiragongo, East Africa
(*Wauthier et al., 2018*)

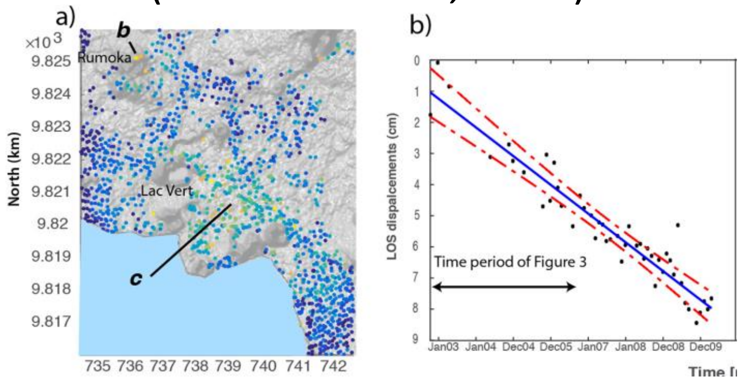

Volcano deflation

Possible mechanisms for continuing post-eruptive subsidence:

- ✓ Viscoelastic relaxation (*Galgana et al., 2014; Segall, 2016; Fujiwara et al., 2018; Yamasaki et al., 2018*);
- ✓ Cooling of lava/magma (*Furuya 2005; Parker et al., 2014; Chaussard 2014*);
- ✓ Pore pressure decrease (*Lu et al., 2002; Wauthier et al., 2018*);
- ✓ Degassing (*Wauthier et al., 2018*);
- ✓ Tectonic extension (*Parker et al., 2014*);

Monitoring and interpreting volcano deflation may provide insights into underground magma process and rheology of host rock.

Usu volcano (Hokkaido, Japan)

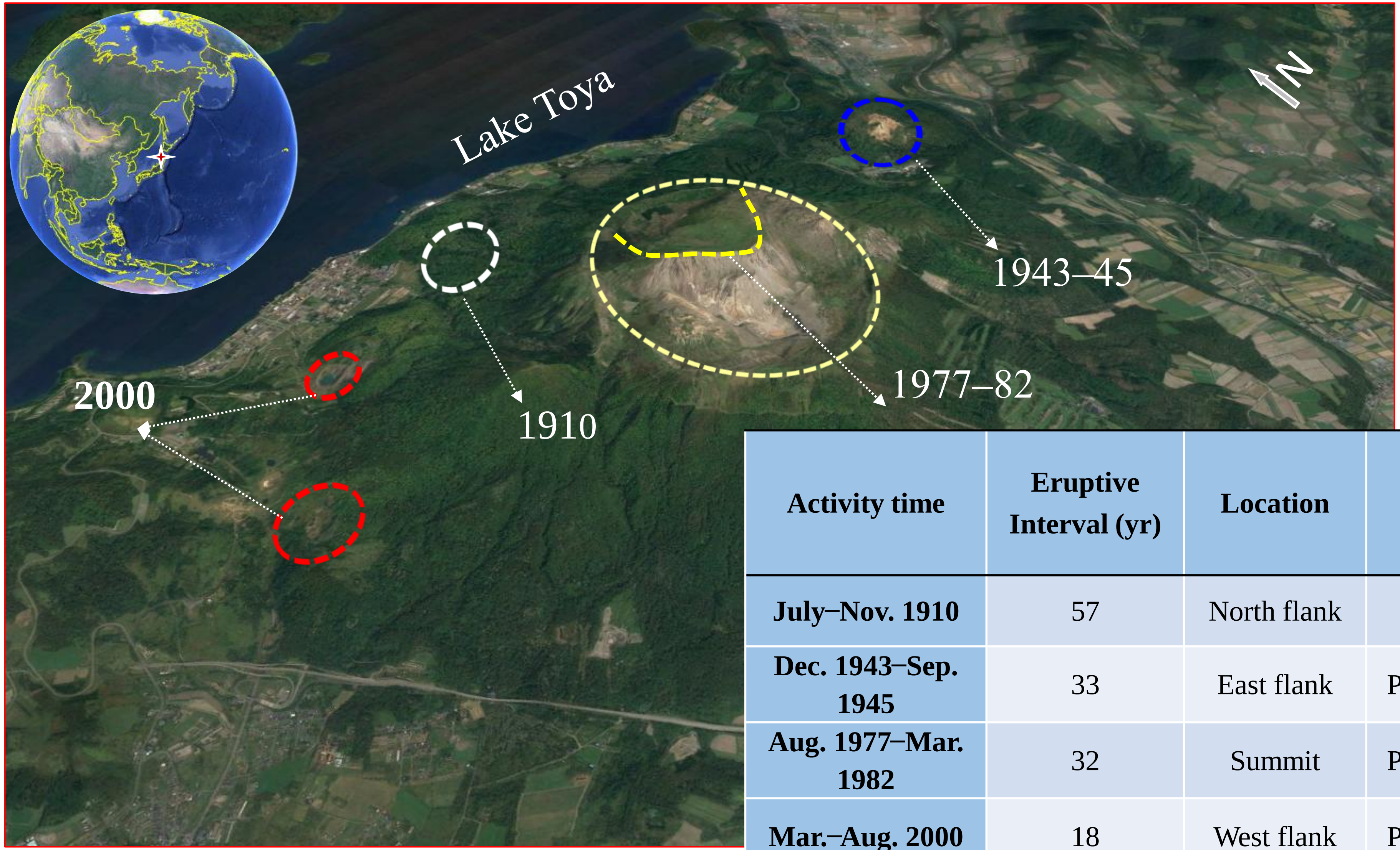

Intermediate eruptive cycle

Activity time	Eruptive Interval (yr)	Location	Eruption type	Upheaval height (m)
July–Nov. 1910	57	North flank	Phreatic	170
Dec. 1943–Sep. 1945	33	East flank	Phreatomagmatic	280
Aug. 1977–Mar. 1982	32	Summit	Phreatomagmatic	180
Mar.–Aug. 2000	18	West flank	Phreatomagmatic	80

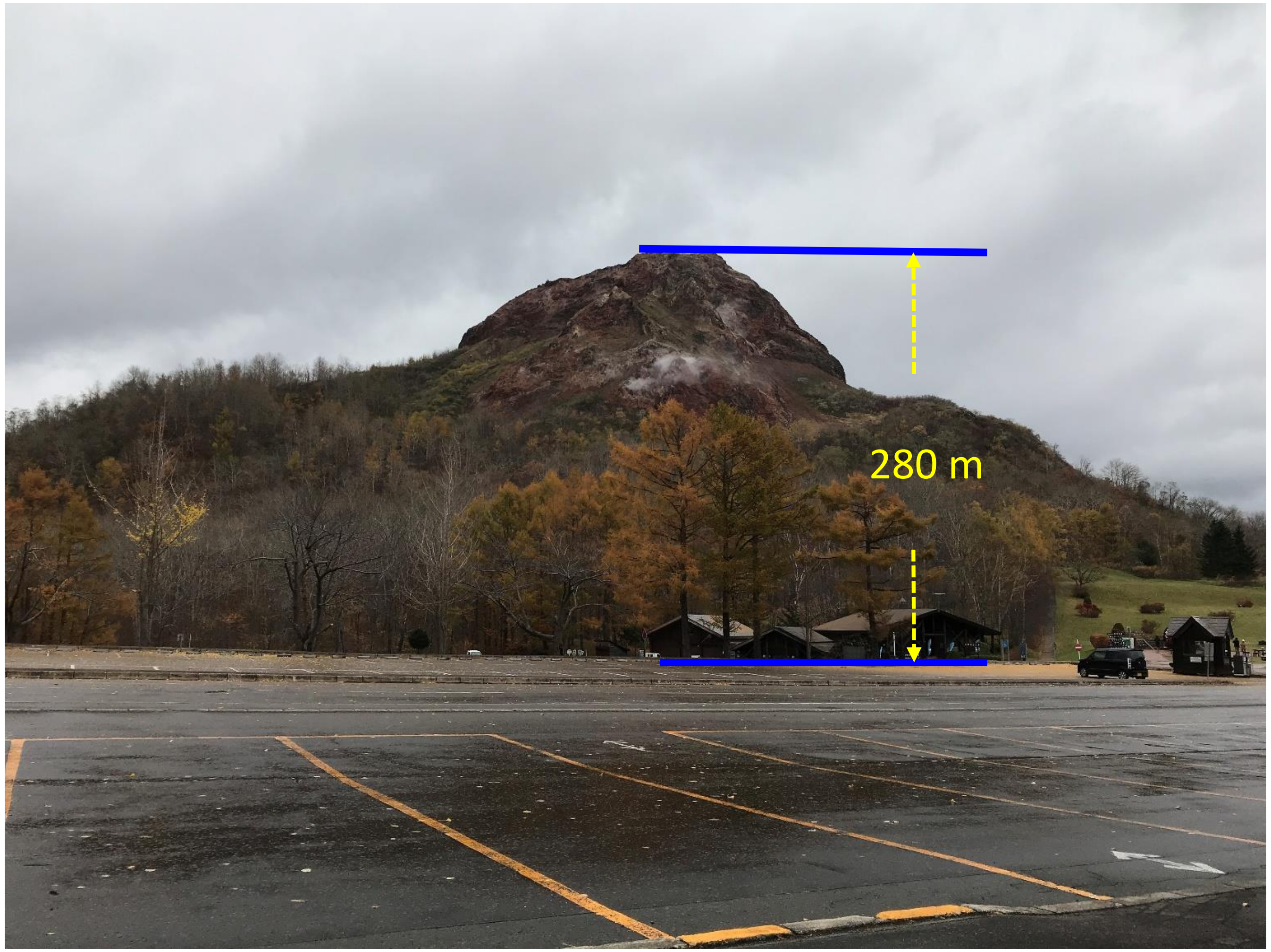

Showa-Shinzan, a lava dome emerged during the 1943—1945 eruption.

The 2000 phreatomagmatic eruption of Usu volcano

Usu volcano: our motivation

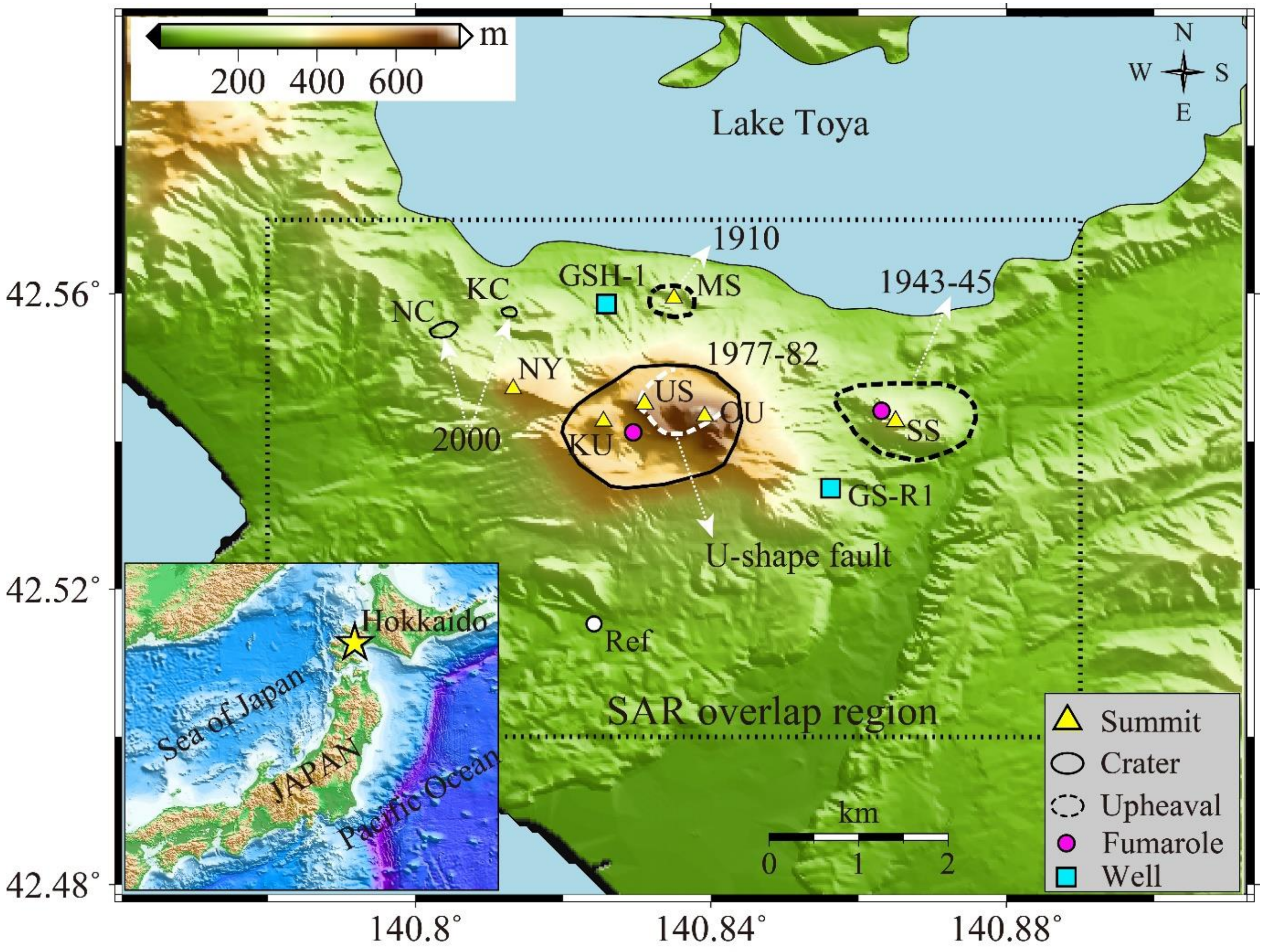

NC: Nishiyama Crater; KC: Konpirayama Crater;

MS: Meiji-Shinzan; SS: Showa-Shinzan; KO: Ko-Usu; US: Usu-Shinzan; OU: O-Usu;

(Yokoyama & Seino, 2000)

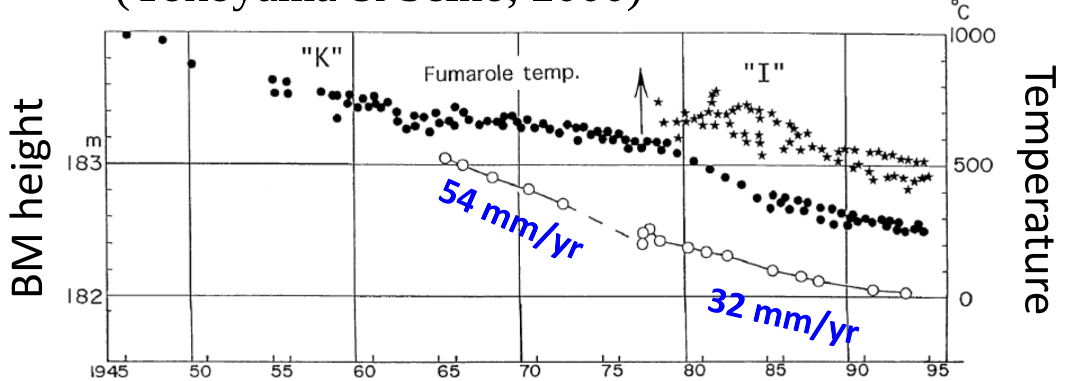

- ✓ Secular subsidence has been reported since 1960s;
- ✓ The mechanism of subsidence has not been well understood;
- ✓ We attempt to investigate the post-eruptive deformation using InSAR;

SAR data

SAR sensor	**JERS-1 (1992-1998)**	**ALOS-1 PALSAR-1 (2006-2011)**		**ALOS-2 PALSAR-2 (2014-2017)**	
Path No.	Path 65, Desc.	Path 401, Asc.	Path 58, Desc.	Path 124, Asc.	Path 19, Desc.
Image Num.	46	20	22	11	12
Interf. Num.	76	72	79	55	66
Interf. Num. for Stacking/SBAS	**53**	**25**	**54**	**50**	**57**
Range (m) × Azimuth (m)	8.8 × 4.5	4.7 × 3.1		1.4 × 1.8	

SAR data processing

- ✓ Used the **GAMMA software** to process the SAR images and generate more than 200 interferograms;
- ✓ Applied the **stacking method** (*Sandwell, 1998*) to the JERS data;
- ✓ Applied the **Small Baseline Subset** method (*Berardino et al., 2001*) to the ALOS-1/2 data;
- ✓ Decomposed the LOS displacements into quasi- vertical and E-W directions.

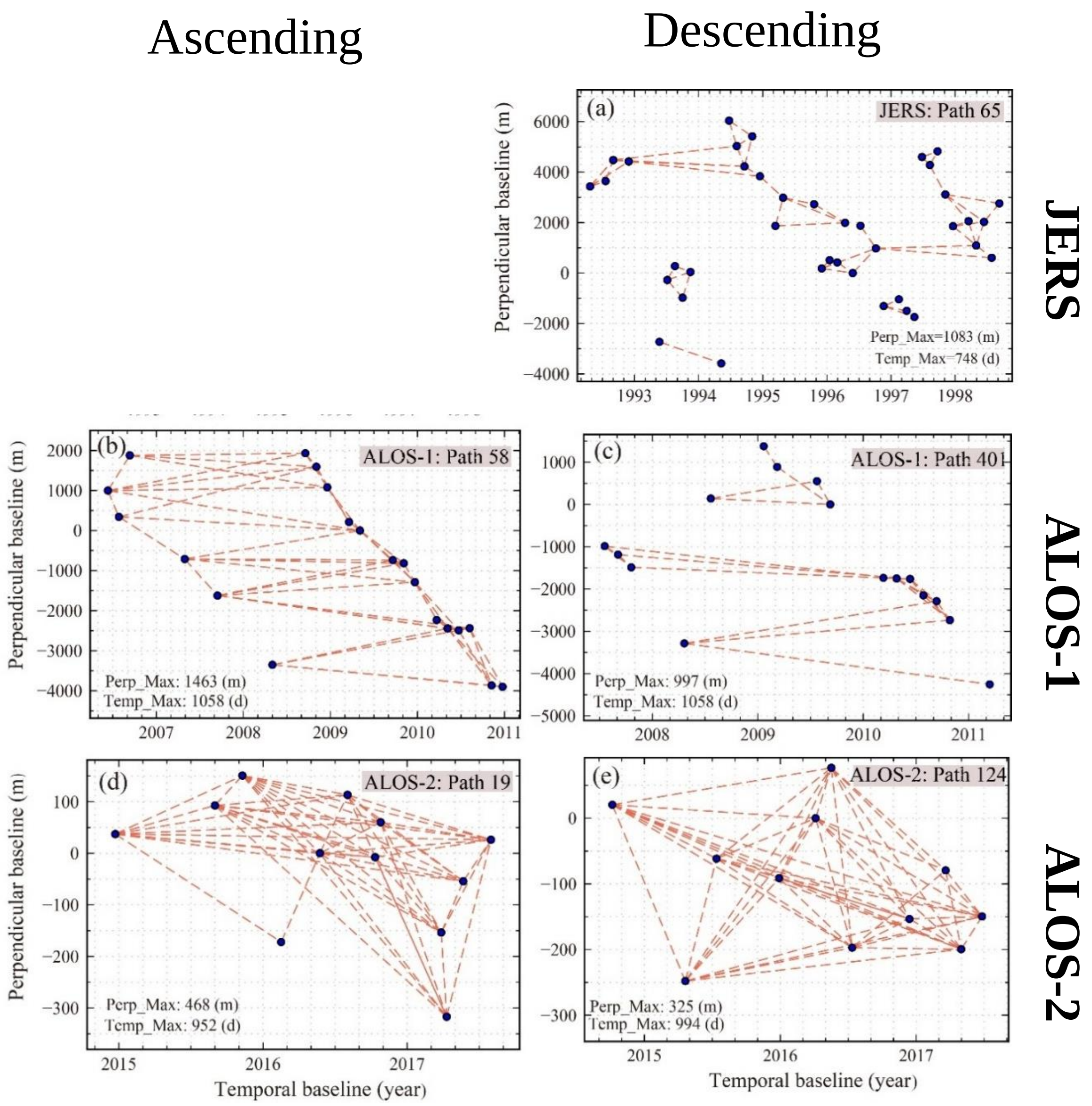

Results: mean LOS velocity

✓ **2000 site:**

- Two sub-regions: NC and KC craters;
- Maximum ALOS-1 velocity: 38 mm/yr;
- Nearly disappear in ALOS-2 measurements;

✓ **1977 site:**

- Has the largest deformation extent;
- Maximum velocities: 66, 45 and 43 mm/yr for the JERS, ALOS-1 and ALOS-2, respectively;

✓ **1943 site:**

- Steady pattern of deformation;
- LOS velocity : ~ 20 mm/yr.

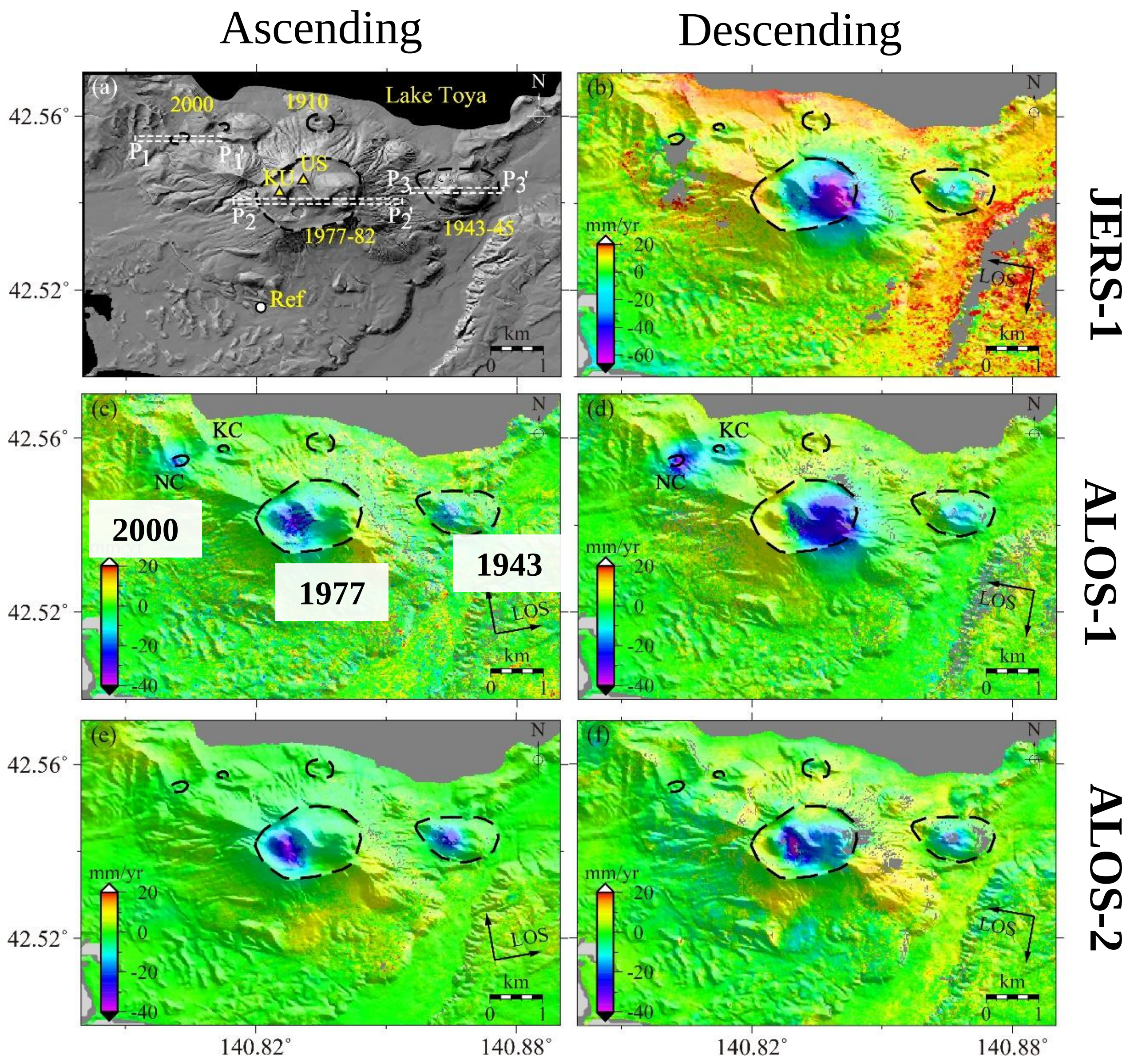

Results: quasi- E-W and U-D mean velocity

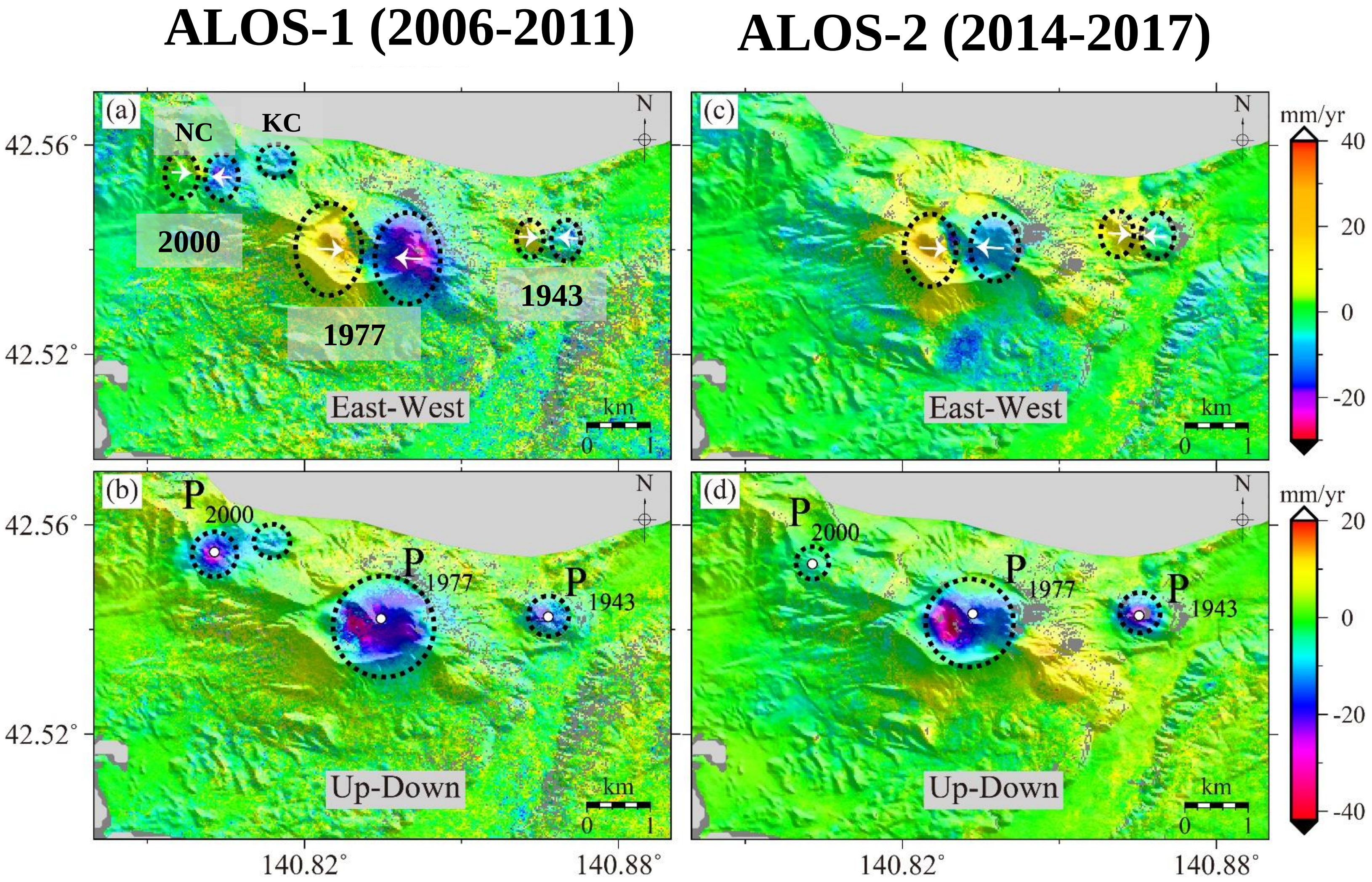

- All the three deformation sites show E-W contraction and vertical subsidence;
- Both the E-W and U-D deformation regions have shrank from 2006 to 2017;
- Maximum subsidence rate : ~ 40 mm/yr at the 1977 eruption site;

Results: displacement temporal evolution

Vertical mean velocity

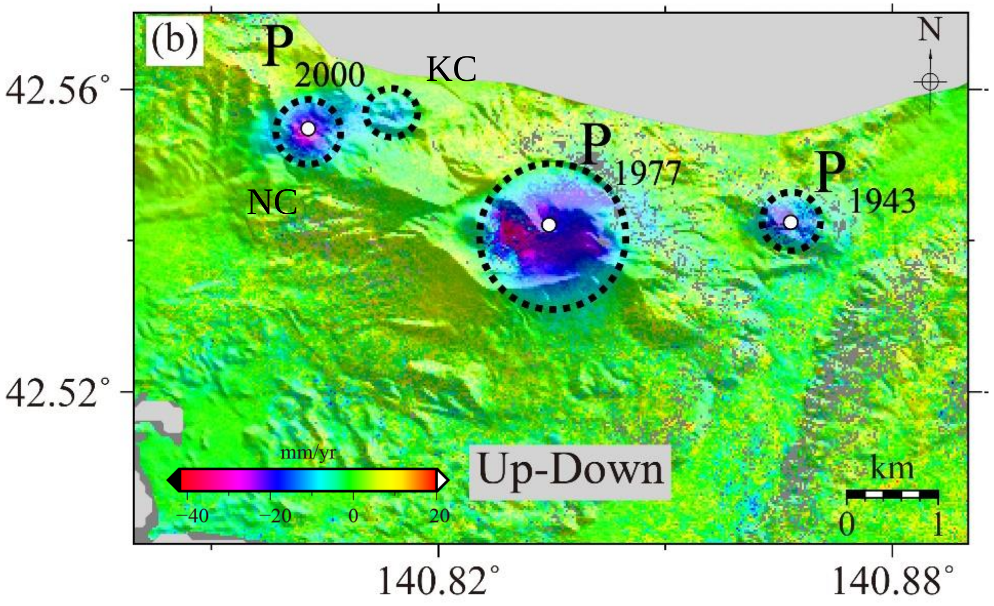

Subsidence rates at the three points

Points	JERS (mm/yr)	ALOS-1 (mm/yr)	ALOS-2 (mm/yr)
P_{2000}	-	-22	-6
P_{1977}	-68	-27	- 24
P_{1943}	-18	-16	-15

✓ The 2000 vent: Drastic decline in subsidence rate.

✓ The 1977 vent: Gradual decline of subsidence.

✓ The 1943 vent: Steady subsidence.

Cooling of intruded magma?

- Localized deformation at vents;
- Deformation area shrinks over time;
- Temporal decay in subsidence rate;

Thermoelastic modeling

Assuming the deformation is caused by an instantaneous spherical heat source in an elastic half–space (***Furuya, 2004; 2005***), the displacement ***u*** at the ground point ***x*** and the time ***t*** can be expressed as :

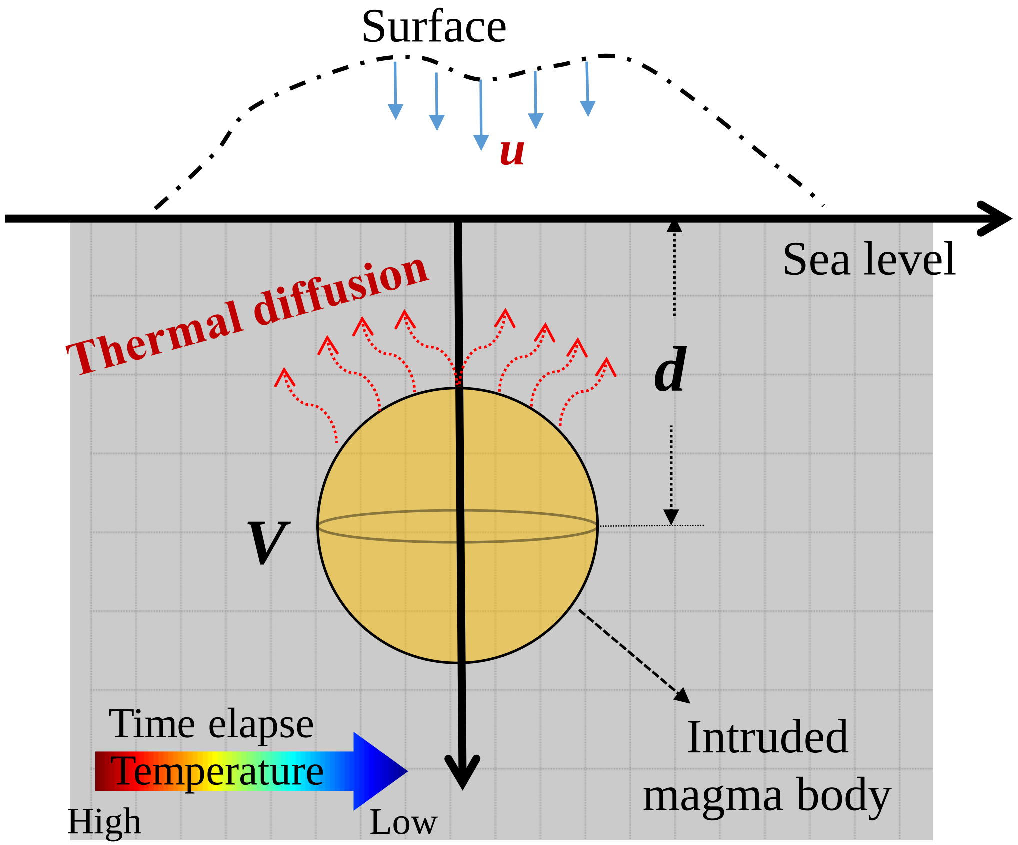

$$\boldsymbol{u}(x, t) = \boldsymbol{f}\,(x, t, V, \mathbf{d}, T, a, k, v)$$

V: source volume ;

d: depth of the source;

T: magma temperature (1200 K);

a: thermal expansivity (2×10^{-5});

k: thermal diffusivity;

v: poisson ratio (0.25);

Thermoelastic modeling

Model initialization:

$$\boldsymbol{d} = \mathbf{G}{*}\boldsymbol{m} + \boldsymbol{\varepsilon}$$

Misfit function:

$$\Gamma = \sqrt{\boldsymbol{r}^T \boldsymbol{C}^{-1} \boldsymbol{r}/(n-p)}$$

$$\boldsymbol{r} = \boldsymbol{d} - \boldsymbol{f}(\boldsymbol{m})$$

m: source parameters (*lon, lat, d, V, k)*

d: mean LOS or vertical velocities

G: Green function from the model

***ε*:** model residual

C: weighting matrix

n: number of observations in ***d***

p: number of source parameters

- We assumed four heat sources and used the mean velocities to constrain the parameters;
- Each dataset was weighted by its observation time-span;

Source parameters

Table below: best fitting model parameters with their 2σ uncertainties.

	Longitude (°)	**Latitude (°)**	**Depth (m b.s.l)**	**Volume ($\times10^6$ m^3)**	**Thermal diffusivity ($\times10^{-5}$ m^2/s)**	**Misfit**	**Data source**
2000 site	140.8034	42.5541	213±19	6.67±0.21	8.21±1.01	2.78	ALOS-1 (NC)
	140.8118	42.5563	100±13	2.05±0.13	8.06±1.20	2.02	ALOS-1 (KC)
1977 site	140.8353	42.5416	396±29	132.18±5.21	10.05±1.09	5.06	JERS+ALOS-1+ALOS-2
1943 site	140.8662	42.5426	92±12	49.51±2.12	1.65±0.22	1.03	JERS+ALOS-1+ALOS-2

- ✓ Four shallow heat sources in depths not deeper than 400 m (b.s.l.);
- ✓ Radii for the four heat sources are 117, 79, 316, and 228 m, respectively;
- ✓ Thermal diffusivity is much higher than the empirical value (0.1–1×10^{-5} m^2/s) ;

Model evaluation

2000 vent

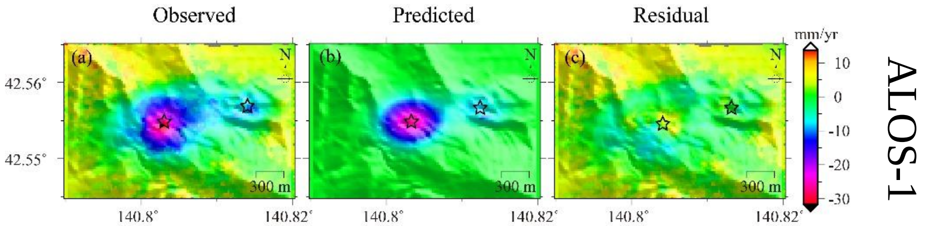

1977 vent

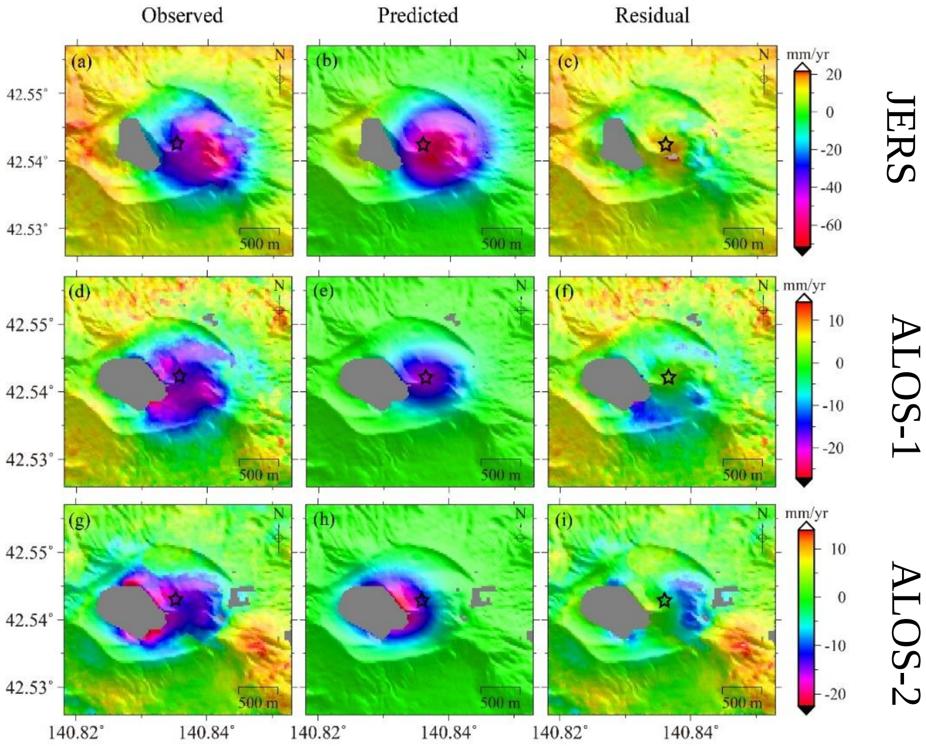

- ✓ Maximum RMS of the residuals for the 2000, 1977 and 1943 sites are 4.17, 6.98, and 3.22 mm/yr, respectively;
- ✓ The thermoelastic models successfully explain the observed post-eruptive deformation;

1943 vent

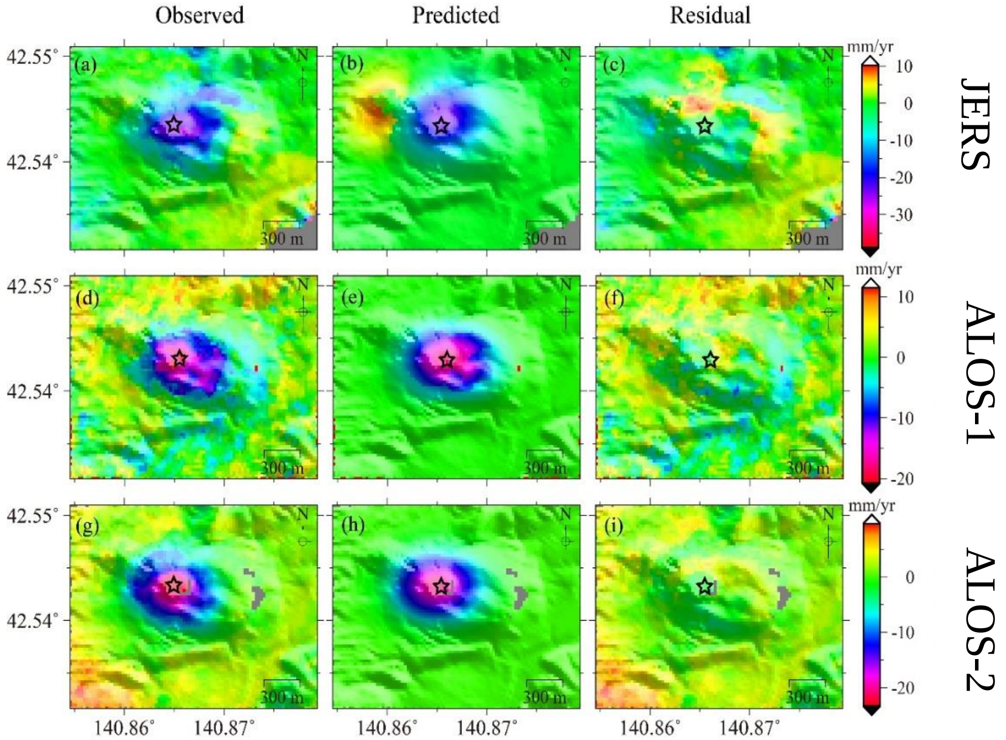

Temporal evolution of vertical displacements : Point P_{1943}

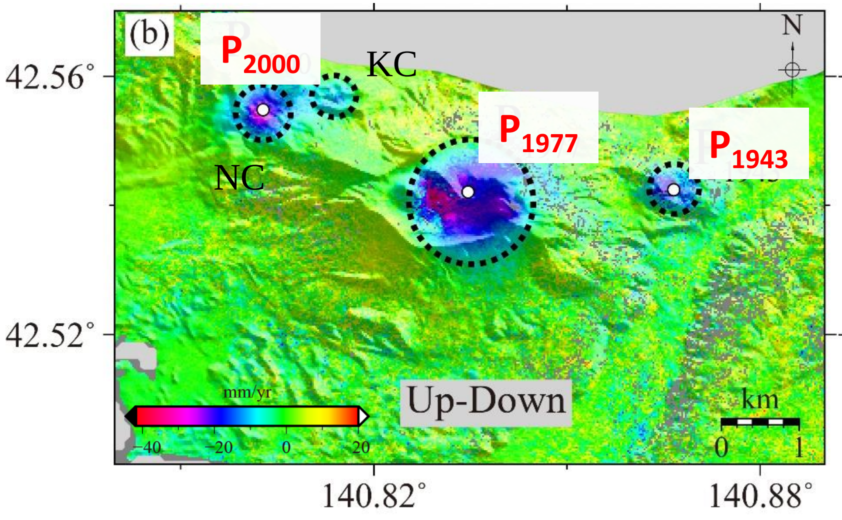

Vertical velocity map

Simulated *vs* Observations

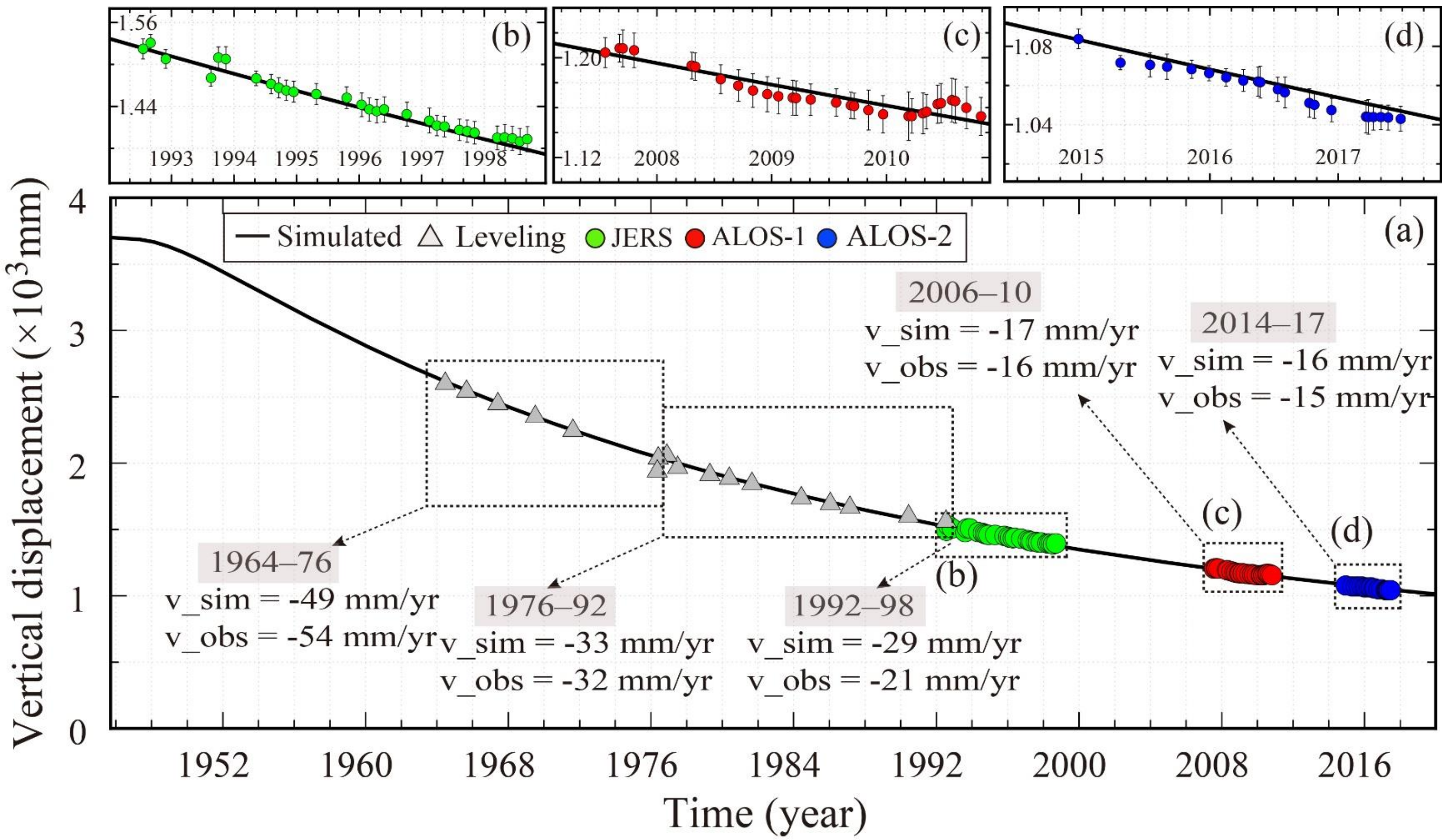

Temporal evolution of vertical displacements : Point P_{1977}

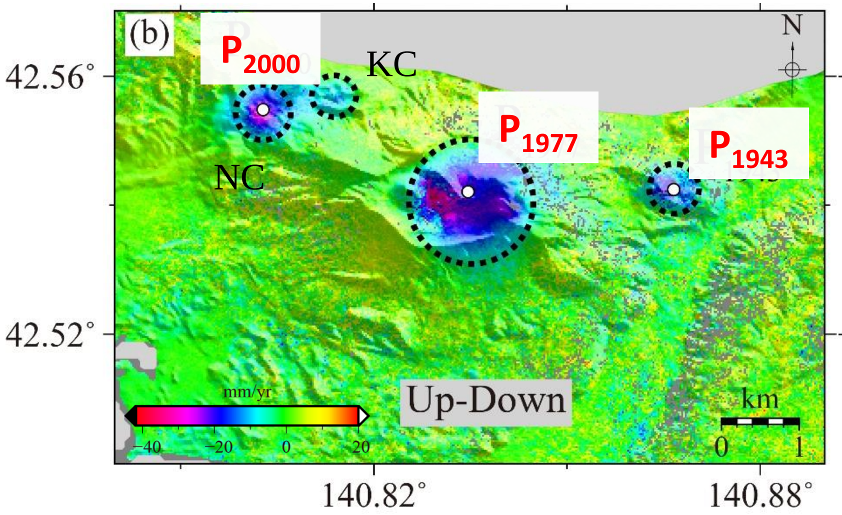

Vertical velocity map

Simulated *vs* Observations

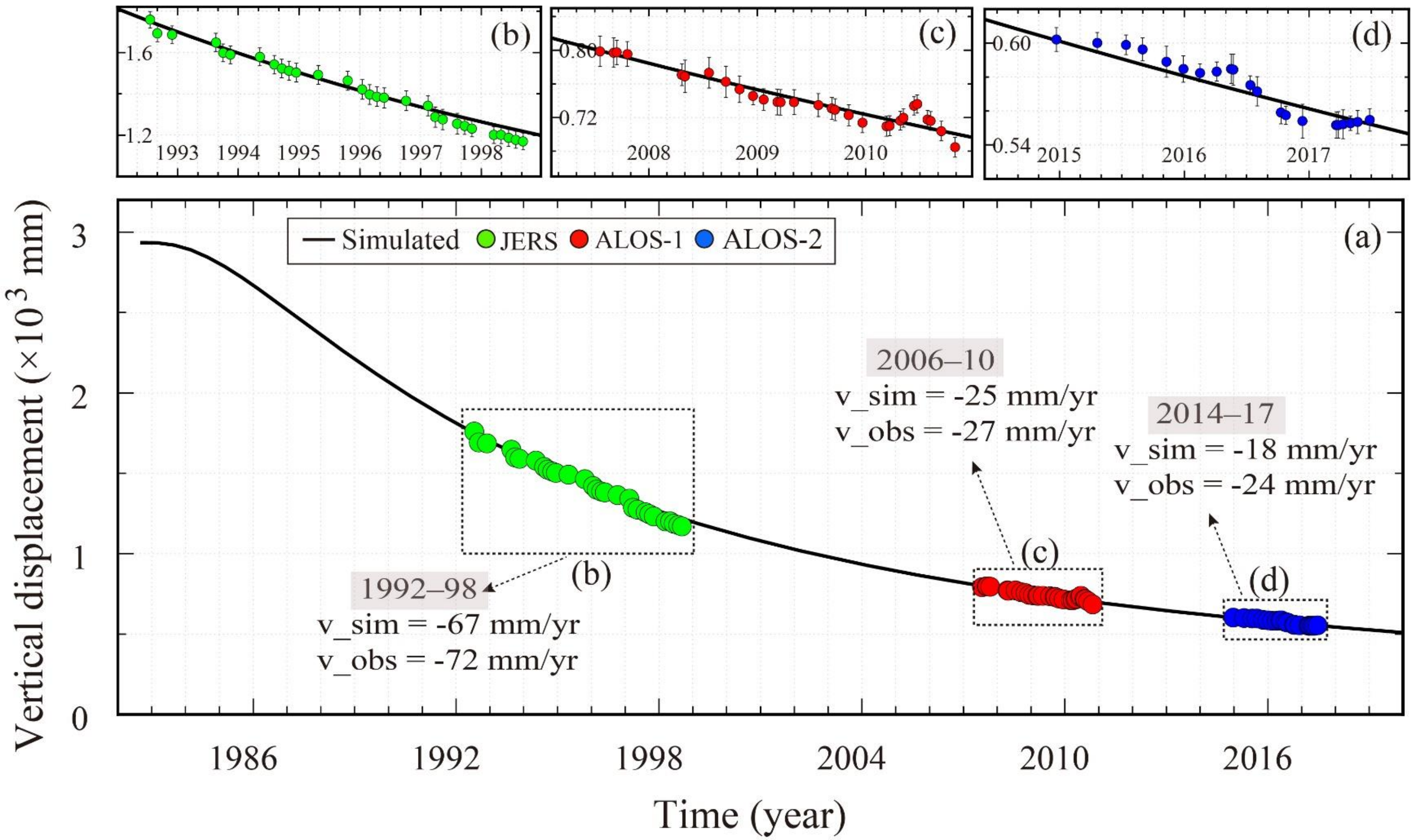

Temporal evolution of vertical displacements : Point P_{2000}

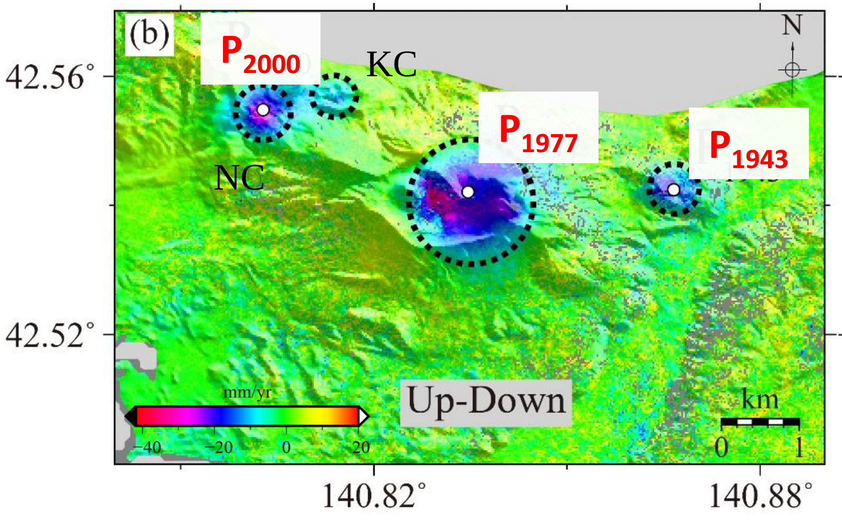

Vertical velocity map

Simulated *vs* Observations

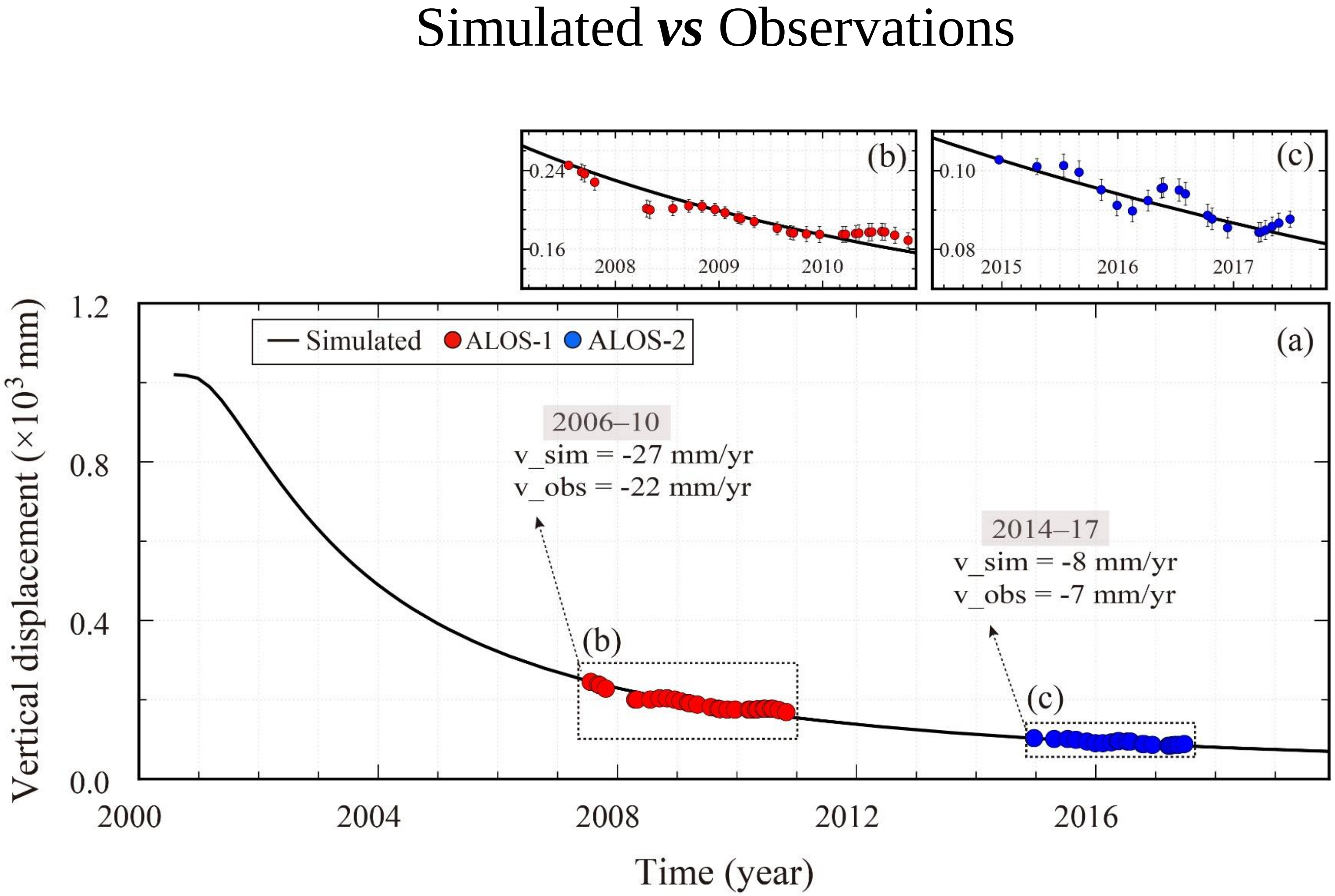

Comparison with resistivity structure

Magnetotelluric (MT) surveying

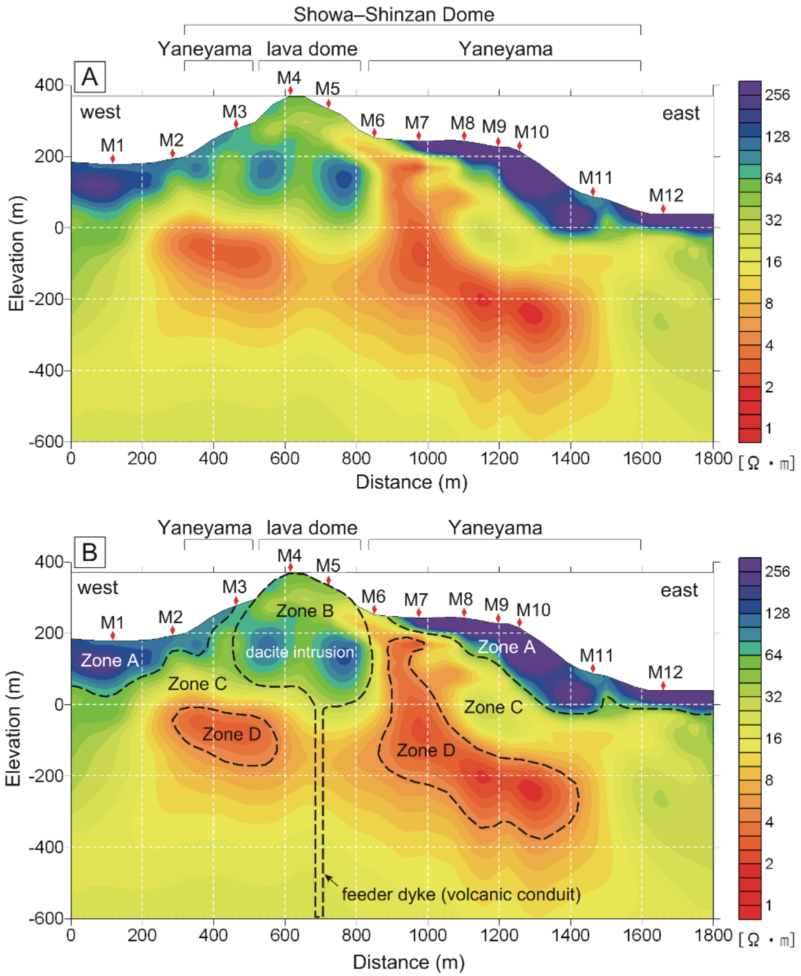

The 1943 vent (*Goto & Johmori, 2014*)

The 1977 vent (*Matsushima et al., 2002; Matsushima, 2003*)

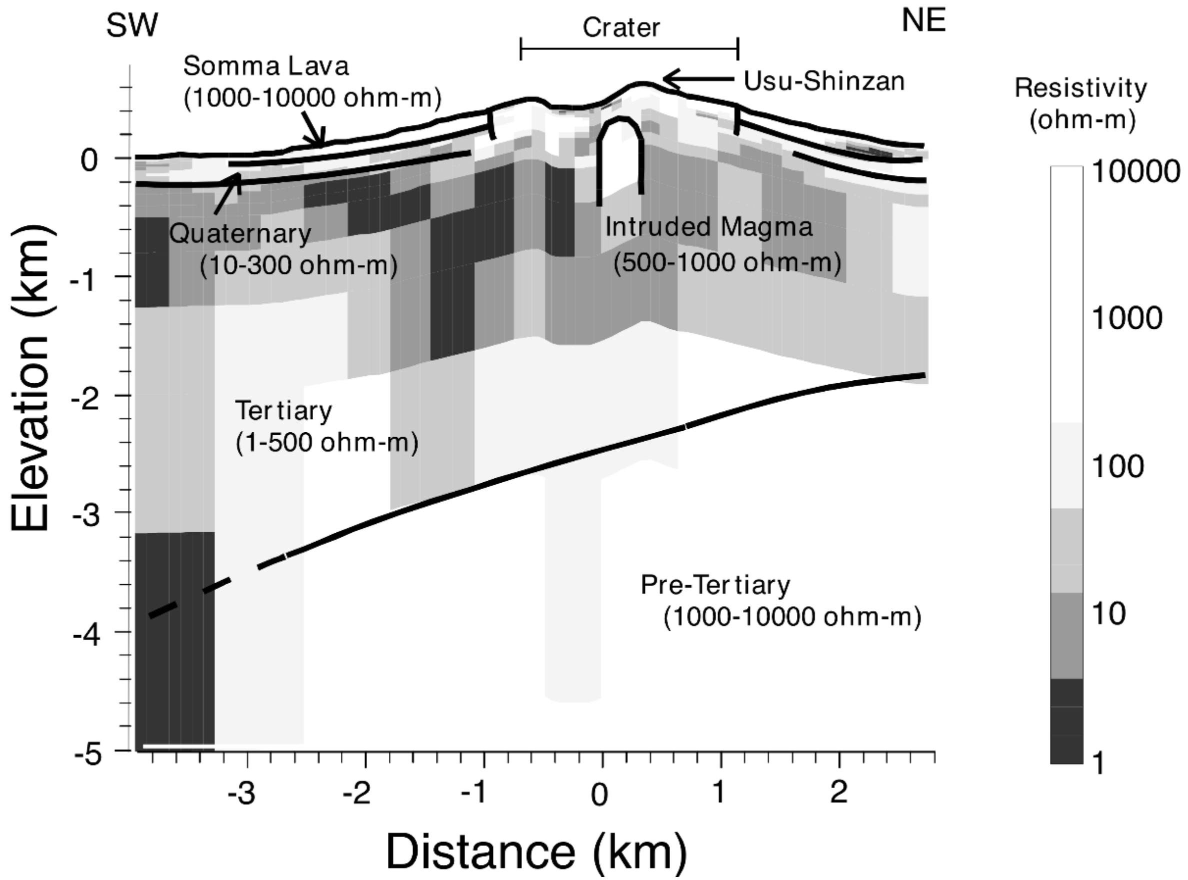

High thermal diffusivity?

✓ **Our modeling results:**

- High apparent thermal diffusivity (10^{-4}~10^{-5} m^2/s), which are 1–2 orders higher than laboratory derived values;
- If we fix the thermal diffusivity with 1×10^{-6} m^2/s, the best-fitting depth and volume for the 1977: 1040 m b.s.l. and 10.42 km^3, respectively.

✓ **Factors influencing thermal diffusivity:**

- Rock temperature
- Pressure
- Degree of water saturation
- Porosity

Lab experiments shown that thermal diffusivity may vary **as much as a factor of two to three** by changing the values of these factors (*Clauser and Huenges*, *2013*) .

High thermal diffusivity?

Groundwater may play an important role in influencing the cooling process :

- Toya lake is right next to the volcano;
- Planetary earthquake swarms would generate rich fractures/faults (*Jousset, 1999*);
- The presence of high permeable rock (*Matsushima, 2003*);
- Decrease of water level after the eruptions.

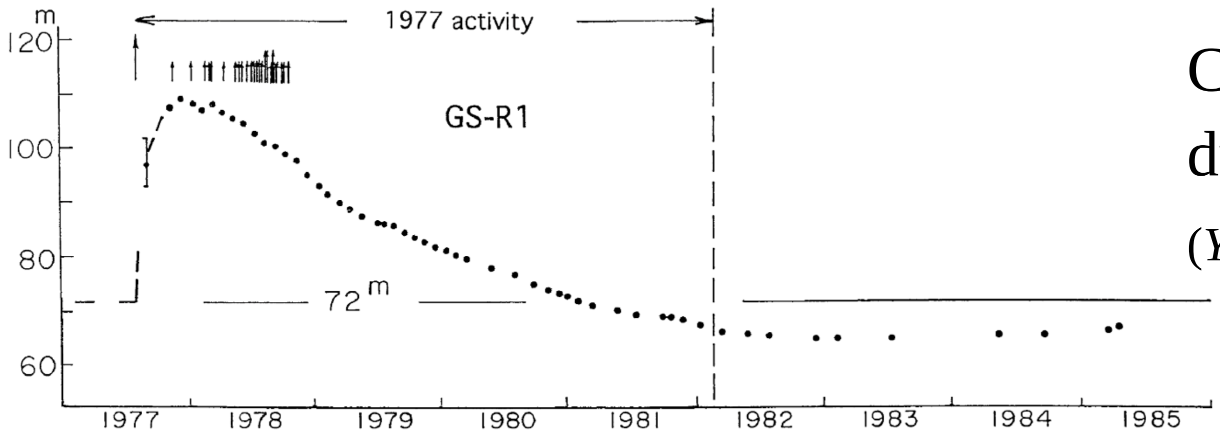

Change of water level during the 1977 eruption

(*Yokoyama and Seino, 2000*)

Conclusions

- ✓ 25 years of InSAR observations at Usu volcano show three deformation regions corresponding to the 2000, 1977 and 1943 eruption sites, respectively;
- ✓ Temporal evolutions of subsidence at the three eruption sites are different from each other;
- ✓ Thermoelastic modeling reveal four shallow heat sources at <400 m below sea level;
- ✓ The underground water flow may play an important role in effectively cooling the volcano.

Thank you for your attention!

Email: insarwxw@eri.u-tokyo.ac.jp